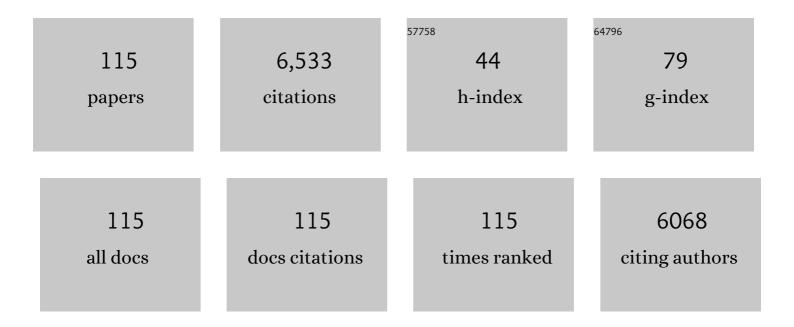
List of Publications by Year in descending order

Source: https://exaly.com/author-pdf/6329813/publications.pdf Version: 2024-02-01



#	Article	IF	CITATIONS
1	Remote sensing of solar-induced chlorophyll fluorescence: Review of methods and applications. Remote Sensing of Environment, 2009, 113, 2037-2051.	11.0	640
2	Evaluation of Sentinel-2 Red-Edge Bands for Empirical Estimation of Green LAI and Chlorophyll Content. Sensors, 2011, 11, 7063-7081.	3.8	410
3	Machine learning regression algorithms for biophysical parameter retrieval: Opportunities for Sentinel-2 and -3. Remote Sensing of Environment, 2012, 118, 127-139.	11.0	400
4	Robust support vector method for hyperspectral data classification and knowledge discovery. IEEE Transactions on Geoscience and Remote Sensing, 2004, 42, 1530-1542.	6.3	236
5	Multioutput Support Vector Regression for Remote Sensing Biophysical Parameter Estimation. IEEE Geoscience and Remote Sensing Letters, 2011, 8, 804-808.	3.1	235
6	A red-edge spectral index for remote sensing estimation of green LAI over agroecosystems. European Journal of Agronomy, 2013, 46, 42-52.	4.1	214
7	Sunâ€induced fluorescence – a new probe of photosynthesis: First maps from the imaging spectrometerÂ <i>HyPlant</i> . Clobal Change Biology, 2015, 21, 4673-4684.	9.5	213
8	Retrieval of Vegetation Biophysical Parameters Using Gaussian Process Techniques. IEEE Transactions on Geoscience and Remote Sensing, 2012, 50, 1832-1843.	6.3	201
9	Red and far red Sunâ€induced chlorophyll fluorescence as a measure of plant photosynthesis. Geophysical Research Letters, 2015, 42, 1632-1639.	4.0	171
10	Highly reliable energy-saving mac for wireless body sensor networks in healthcare systems. IEEE Journal on Selected Areas in Communications, 2009, 27, 553-565.	14.0	159
11	Improved Fraunhofer Line Discrimination Method for Vegetation Fluorescence Quantification. IEEE Geoscience and Remote Sensing Letters, 2008, 5, 620-624.	3.1	158
12	Multitemporal fusion of Landsat/TM and ENVISAT/MERIS for crop monitoring. International Journal of Applied Earth Observation and Geoinformation, 2013, 23, 132-141.	2.8	125
13	Retrieval of sun-induced fluorescence using advanced spectral fitting methods. Remote Sensing of Environment, 2015, 169, 344-357.	11.0	119
14	Estimation of solar-induced vegetation fluorescence from space measurements. Geophysical Research Letters, 2007, 34, .	4.0	118
15	CEFLES2: the remote sensing component to quantify photosynthetic efficiency from the leaf to the region by measuring sun-induced fluorescence in the oxygen absorption bands. Biogeosciences, 2009, 6, 1181-1198.	3.3	115
16	Angular Dependency of Hyperspectral Measurements over Wheat Characterized by a Novel UAV Based Goniometer. Remote Sensing, 2015, 7, 725-746.	4.0	109
17	A RADARSAT-2 Quad-Polarized Time Series for Monitoring Crop and Soil Conditions in Barrax, Spain. IEEE Transactions on Geoscience and Remote Sensing, 2012, 50, 1057-1070.	6.3	102
18	Goodbye, ALOHA!. IEEE Access, 2016, 4, 2029-2044.	4.2	101

#	Article	IF	CITATIONS
19	Bidirectional sun-induced chlorophyll fluorescence emission is influenced by leaf structure and light scattering properties — A bottom-up approach. Remote Sensing of Environment, 2015, 158, 169-179.	11.0	99
20	Remote sensing of sunlight-induced chlorophyll fluorescence and reflectance of Scots pine in the boreal forest during spring recovery. Remote Sensing of Environment, 2005, 96, 37-48.	11.0	98
21	A Survey on M2M Systems for mHealth: A Wireless Communications Perspective. Sensors, 2014, 14, 18009-18052.	3.8	98
22	Optimizing LUT-Based RTM Inversion for Semiautomatic Mapping of Crop Biophysical Parameters from Sentinel-2 and -3 Data: Role of Cost Functions. IEEE Transactions on Geoscience and Remote Sensing, 2014, 52, 257-269.	6.3	97
23	Developments for vegetation fluorescence retrieval from spaceborne highâ€resolution spectrometry in the O ₂ â€A and O ₂ â€B absorption bands. Journal of Geophysical Research, 2010, 115, .	3.3	92
24	Gaussian Process Retrieval of Chlorophyll Content From Imaging Spectroscopy Data. IEEE Journal of Selected Topics in Applied Earth Observations and Remote Sensing, 2013, 6, 867-874.	4.9	92
25	How Universal Is the Relationship between Remotely Sensed Vegetation Indices and Crop Leaf Area Index? A Global Assessment. Remote Sensing, 2016, 8, 597.	4.0	91
26	A method for the surface reflectance retrieval from PROBA/CHRIS data over land: application to ESA SPARC campaigns. IEEE Transactions on Geoscience and Remote Sensing, 2005, 43, 2908-2917.	6.3	90
27	Upward and downward solar-induced chlorophyll fluorescence yield indices of four tree species as indicators of traffic pollution in Valencia. Environmental Pollution, 2013, 173, 29-37.	7.5	89
28	Estimating chlorophyll content of crops from hyperspectral data using a normalized area over reflectance curve (NAOC). International Journal of Applied Earth Observation and Geoinformation, 2010, 12, 165-174.	2.8	88
29	Plant chlorophyll fluorescence: active and passive measurements at canopy and leaf scales with different nitrogen treatments. Journal of Experimental Botany, 2016, 67, 275-286.	4.8	82
30	Correction of systematic spatial noise in push-broom hyperspectral sensors: application to CHRIS/PROBA images. Applied Optics, 2008, 47, F46.	2.1	78
31	Gaussian processes retrieval of leaf parameters from a multi-species reflectance, absorbance and fluorescence dataset. Journal of Photochemistry and Photobiology B: Biology, 2014, 134, 37-48.	3.8	70
32	Information Exchange in Randomly Deployed Dense WSNs With Wireless Energy Harvesting Capabilities. IEEE Transactions on Wireless Communications, 2016, 15, 3008-3018.	9.2	70
33	Wireless Energy Harvesting in Two-Way Network Coded Cooperative Communications: A Stochastic Approach for Large Scale Networks. IEEE Communications Letters, 2014, 18, 1011-1014.	4.1	69
34	Diurnal Cycle Relationships between Passive Fluorescence, PRI and NPQ of Vegetation in a Controlled Stress Experiment. Remote Sensing, 2017, 9, 770.	4.0	67
35	Sun-Induced Chlorophyll Fluorescence II: Review of Passive Measurement Setups, Protocols, and Their Application at the Leaf to Canopy Level. Remote Sensing, 2019, 11, 927.	4.0	61
36	Evaluation of remote sensing of vegetation fluorescence by the analysis of diurnal cycles. International Journal of Remote Sensing, 2008, 29, 5423-5436.	2.9	59

#	Article	IF	CITATIONS
37	Multiobjective Auction-Based Switching-Off Scheme in Heterogeneous Networks: To Bid or Not to Bid?. IEEE Transactions on Vehicular Technology, 2016, 65, 9168-9180.	6.3	59
38	Early Diagnosis of Vegetation Health From High-Resolution Hyperspectral and Thermal Imagery: Lessons Learned From Empirical Relationships and Radiative Transfer Modelling. Current Forestry Reports, 2019, 5, 169-183.	7.4	58
39	Sun-Induced Chlorophyll Fluorescence III: Benchmarking Retrieval Methods and Sensor Characteristics for Proximal Sensing. Remote Sensing, 2019, 11, 962.	4.0	57
40	Device-to-device communications and small cells: enabling spectrum reuse for dense networks. IEEE Wireless Communications, 2014, 21, 98-105.	9.0	54
41	The High-Performance Airborne Imaging Spectrometer HyPlant—From Raw Images to Top-of-Canopy Reflectance and Fluorescence Products: Introduction of an Automatized Processing Chain. Remote Sensing, 2019, 11, 2760.	4.0	53
42	Scene-based spectral calibration assessment of high spectral resolution imaging spectrometers. Optics Express, 2009, 17, 11594.	3.4	49
43	A near-optimum cross-layered distributed queuing protocol for wireless LAN. IEEE Wireless Communications, 2008, 15, 48-55.	9.0	44
44	Compensation of Oxygen Transmittance Effects for Proximal Sensing Retrieval of Canopy–Leaving Sun–Induced Chlorophyll Fluorescence. Remote Sensing, 2018, 10, 1551.	4.0	44
45	FLEX End-to-End Mission Performance Simulator. IEEE Transactions on Geoscience and Remote Sensing, 2016, 54, 4215-4223.	6.3	42
46	Dynamic energy efficient distance-aware Base Station switch on/off scheme for LTE-advanced. , 2012, , .		37
47	Regularized Multiresolution Spatial Unmixing for ENVISAT/MERIS and Landsat/TM Image Fusion. IEEE Geoscience and Remote Sensing Letters, 2011, 8, 844-848.	3.1	35
48	A Cloud-Assisted Random Linear Network Coding Medium Access Control Protocol for Healthcare Applications. Sensors, 2014, 14, 4806-4830.	3.8	35
49	Variability and Uncertainty Challenges in Scaling Imaging Spectroscopy Retrievals and Validations from Leaves Up to Vegetation Canopies. Surveys in Geophysics, 2019, 40, 631-656.	4.6	35
50	Spatial Variation of Leaf Optical Properties in a Boreal Forest Is Influenced by Species and Light Environment. Frontiers in Plant Science, 2017, 8, 309.	3.6	32
51	Sun-Induced Chlorophyll Fluorescence I: Instrumental Considerations for Proximal Spectroradiometers. Remote Sensing, 2019, 11, 960.	4.0	31
52	First Results From the PROBA/CHRIS Hyperspectral/Multiangular Satellite System Over Land and Water Targets. IEEE Geoscience and Remote Sensing Letters, 2005, 2, 250-254.	3.1	30
53	Standardized Low-Power Wireless Communication Technologies for Distributed Sensing Applications. Sensors, 2014, 14, 2663-2682.	3.8	27
54	The 2013 FLEX—US Airborne Campaign at the Parker Tract Loblolly Pine Plantation in North Carolina, USA. Remote Sensing, 2017, 9, 612.	4.0	27

#	Article	IF	CITATIONS
55	On Hyperspectral Remote Sensing of Leaf Biophysical Constituents: Decoupling Vegetation Structure and Leaf Optics Using CHRIS–PROBA Data Over Crops in Barrax. IEEE Geoscience and Remote Sensing Letters, 2014, 11, 1579-1583.	3.1	26
56	LPDQ: A self-scheduled TDMA MAC protocol for one-hop dynamic low-power wireless networks. Pervasive and Mobile Computing, 2015, 20, 84-99.	3.3	26
57	A field study on solar-induced chlorophyll fluorescence and pigment parameters along a vertical canopy gradient of four tree species in an urban environment. Science of the Total Environment, 2014, 466-467, 185-194.	8.0	25
58	In vivo photoprotection mechanisms observed from leaf spectral absorbance changes showing VIS–NIR slow-induced conformational pigment bed changes. Photosynthesis Research, 2019, 142, 283-305.	2.9	22
59	Gridding Artifacts on Medium-Resolution Satellite Image Time Series: MERIS Case Study. IEEE Transactions on Geoscience and Remote Sensing, 2011, 49, 2601-2611.	6.3	21
60	Design and Analysis of an Energy-Saving Distributed MAC Mechanism for Wireless Body Sensor Networks. Eurasip Journal on Wireless Communications and Networking, 2010, 2010, .	2.4	20
61	Model based compressed sensing reconstruction algorithms for ECG telemonitoring in WBANs. , 2014, 35, 105-116.		20
62	Impact of Atmospheric Inversion Effects on Solar-Induced Chlorophyll Fluorescence: Exploitation of the Apparent Reflectance as a Quality Indicator. Remote Sensing, 2017, 9, 622.	4.0	20
63	Comparative analysis of atmospheric radiative transfer models using the Atmospheric Look-up table Generator (ALG) toolbox (version 2.0). Geoscientific Model Development, 2020, 13, 1945-1957.	3.6	20
64	Design of a Generic 3-D Scene Generator for Passive Optical Missions and Its Implementation for the ESA's FLEX/Sentinel-3 Tandem Mission. IEEE Transactions on Geoscience and Remote Sensing, 2018, 56, 1290-1307.	6.3	16
65	Sensitivity analysis of the fraunhofer line discrimination method for the measurement of chlorophyll fluorescence using a field spectroradiometer. , 2007, , .		15
66	Energy-Efficiency Analysis of a Distributed Queuing Medium Access Control Protocol for Biomedical Wireless Sensor Networks in Saturation Conditions. Sensors, 2011, 11, 1277-1296.	3.8	15
67	Gradient-Based Automatic Lookup Table Generator for Radiative Transfer Models. IEEE Transactions on Geoscience and Remote Sensing, 2019, 57, 1040-1048.	6.3	15
68	Towards a novel approach for Sentinel-3 synergistic OLCI/SLSTR cloud and cloud shadow detection based on stereo cloud-top height estimation. ISPRS Journal of Photogrammetry and Remote Sensing, 2021, 181, 238-253.	11.1	15
69	New Cloud Detection Algorithm for Multispectral and Hyperspectral Images: Application to ENVISAT/MERIS and PROBA/CHRIS Sensors. , 2006, , .		14
70	Sharing the small cells for energy efficient networking: How much does it cost?. , 2014, , .		14
71	Leaf-Level Spectral Fluorescence Measurements: Comparing Methodologies for Broadleaves and Needles. Remote Sensing, 2019, 11, 532.	4.0	14
72	Cross-layer enhancement for wlan systems with heterogeneous traffic based on DQCA. , 2008, 46, 60-66.		13

#	Article	IF	CITATIONS
73	Assessment of Approximations in Aerosol Optical Properties and Vertical Distribution into FLEX Atmospherically-Corrected Surface Reflectance and Retrieved Sun-Induced Fluorescence. Remote Sensing, 2017, 9, 675.	4.0	12
74	Difference and Potential of the Upward and Downward Sun-Induced Chlorophyll Fluorescence on Detecting Leaf Nitrogen Concentration in Wheat. Remote Sensing, 2018, 10, 1315.	4.0	12
75	Performance Analysis of a Cluster-Based MAC Protocol for Wireless Ad Hoc Networks. Eurasip Journal on Wireless Communications and Networking, 2010, 2010, .	2.4	10
76	Cloud detection for CHRIS/Proba hyperspectral images. , 2005, , .		9
77	An Overview of the Regional Experiments for Land-atmosphere Exchanges 2012 (REFLEX 2012) Campaign. Acta Geophysica, 2015, 63, 1465-1484.	2.0	9
78	Study of the diurnal cycle of stressed vegetation for the improvement of fluorescence remote sensing. , 2006, 6359, 156.		7
79	Connectivity Analysis in Wireless-Powered Sensor Networks with Battery-Less Devices. , 2016, , .		7
80	Multitemporal image classification and change detection with kernels. , 2006, 6365, 136.		6
81	CHRIS/Proba Toolbox for hyperspectral and multiangular data exploitations. , 2009, , .		6
82	Impact of Structural, Photochemical and Instrumental Effects on Leaf and Canopy Reflectance Variability in the 500–600 nm Range. Remote Sensing, 2022, 14, 56.	4.0	6
83	Multi-resolution spatial unmixing for MERIS and Landsat image fusion. , 2010, , .		5
84	Relating Hyperspectral Airborne Data to Ground Measurements in a Complex and Discontinuous Canopy. Acta Geophysica, 2015, 63, 1499-1515.	2.0	5
85	Modeling and Analysis of Reservation Frame Slotted-ALOHA in Wireless Machine-to-Machine Area Networks for Data Collection. Sensors, 2015, 15, 3911-3931.	3.8	5
86	Delay and Energy Consumption Analysis of Frame Slotted ALOHA variants for Massive Data Collection in Internet-of-Things Scenarios. Applied Sciences (Switzerland), 2020, 10, 327.	2.5	4
87	Remote sensing of chlorophyll fluorescence for estimation of stress in vegetation. recommendations for future missions. , 2007, , .		3
88	Experimental Energy Consumption of Frame Slotted ALOHA and Distributed Queuing for Data Collection Scenarios. Sensors, 2014, 14, 13416-13436.	3.8	3
89	Reliable Machine-to-Machine Multicast Services with Multi-Radio Cooperative Retransmissions. Mobile Networks and Applications, 2015, 20, 734-744.	3.3	3
90	Combining distributed queuing with energy harvesting to enable perpetual distributed data collection applications. Transactions on Emerging Telecommunications Technologies, 2018, 29, e3195.	3.9	3

#	Article	IF	CITATIONS
91	Misión FLEX (Fluorescence Explorer): Observación de la fluorescencia por teledetección como nueva técnica de estudio del estado de la vegetación terrestre a escala global. Revista De Teledeteccion, 2014,	0.6	3
92	Spatio-spectral deconvolution for high resolution spectral imaging with an application to the estimation of sun-induced fluorescence. Remote Sensing of Environment, 2021, 267, 112718.	11.0	3
93	Modelling spatial and spectral systematic noise patterns on CHRIS/PROBA hyperspectral data. , 2006, , .		2
94	Multitemporal fusion of Landsat and MERIS images. , 2011, , .		2
95	Propagation of spectral characterization errors of imaging spectrometers at level-1 and its correction within a level-2 recalibration scheme. , 2015, , .		2
96	Oxygen transmittance correction for solar-induced chlorophyll fluorescence measured on proximal sensing: Application to the NASA-GSFC fusion tower. , 2017, , .		2
97	Photoprotection Dynamics Observed at Leaf Level from Fast Temporal Reflectance Changes. , 2018, , .		2
98	Robust automatic classification method for hyperspectral imagery. , 2004, 5238, 398.		1
99	Potential retrieval of biophysical parameters from FLORIS, S3-OLCI and its synergy. , 2012, , .		1
100	Optimizing LUT-based radiative transfer model inversion for retrieval of biophysical parameters using hyperspectral data. , 2012, , .		1
101	End-to-end communication challenges in M2M systems for mHealth applications. , 2014, , .		1
102	A sun-induced vegetation fluorescence retrieval method from top of atmosphere radiance for the FLEX/Sentinel-3 TanDEM mission. , 2015, , .		1
103	Novel leaf-level measurements of chlorophyll fluorescence for photosynthetic efficiency. , 2015, , .		1
104	<title>Methodology for quantitative analysis of scaling effects in multiresolution datasets acquired with airborne sensors flying at different altitude levels</title> . , 2001, 4170, 73.		0
105	<title>Direct gradient analysis as a new tool for interpretation of hyperspectral remote sensing data:
application to HYMAP/DAISEX-99 data</title> . , 2001, 4171, 229.		0
106	Remote sensing of sun-induced chlorophyll fluorescence at different scales. , 2014, , .		0
107	A fluorescence retrieval method for the flex sentinel-3 tandem mission. , 2014, , .		0
108	Synthetic scene simulator for hyperspectral spaceborne passive optical sensors. Application to ESA's FLEX/sentinel-3 tandem mission. , 2014, , .		0

#	Article	IF	CITATIONS
109	Efficient Contention Resolution in Highly Dense LTE Networks for Machine Type Communications. , 2014, , .		0
110	Design of a satellite end-to-end mission performance simulator for imaging spectrometers and its application to the ESA's FLEX/Sentinel-3 tandem mission. Proceedings of SPIE, 2015, , .	0.8	0
111	Predicting year of plantation with hyperspectral and lidar data. , 2017, , .		Ο
112	FLEX/S3 Tandem Mission Performance Assessment: Evolution of the End-to-End Simulator Flex-E. , 2018, , .		0
113	Alg: a Toolbox for the Generation of Look-Up tables Based on Atmospheric Radiative Transfer Models. , 2018, , .		0
114	Affine Illumination Compensation on Hyperspectral/Multiangular Remote Sensing Images. Lecture Notes in Computer Science, 2011, , 360-369.	1.3	0
115	Body Sensors and Healthcare Monitoring. Advances in Healthcare Information Systems and Administration Book Series, 2012, , 26-55.	0.2	Ο